Control of spiral turbulence by periodic forcing in a reaction-diffusion system with gradients

Yabi Wu,[1,*] Chun Qiao,[1,*] Qi Ouyang,[1,2,3,†] and HongLi Wang[1,2,3]
[1]*Department of Physics, Peking University, Beijing 100871, China*
[2]*The Beijing-Hong Kong-Singapore Joint Center for Nonlinear and Complex Systems (PKU), Peking University, Beijing 100871, China*
[3]*Center for Theoretical Biology, Peking University, Beijing 100871, China*
(Received 15 August 2007; revised manuscript received 22 October 2007; published 28 March 2008)

We report an experimental result on successfully controlling spiral turbulence in a reaction-diffusion system. The control is realized by periodic forcing in a three-dimensional Belousov-Zhabotinsky reaction-diffusion system, which has chemical concentration gradients in the third dimension. We observe that, in the oscillatory regime of the system, a suitable periodic forcing may stabilize scroll waves (SWs), which otherwise undergo a transition to spiral turbulence. Relating the spiral phase shift due to gradients and the forcing frequency, the mechanism of the control can be well understood by modulating the phase twist of SWs. We use the FitzHugh-Nagumo model to demonstrate this mechanism.

DOI: 10.1103/PhysRevE.77.036226 PACS number(s): 82.40.Ck, 05.45.Gg, 05.45.Pq, 47.54.−r

I. INTRODUCTION

Along with studies of transitions from an ordered structure to spatiotemporal turbulence in a spatially extended system, searches for different control strategies to prevent these transitions have continuously been one of the focuses in nonlinear science [1–8]. Among them, the control of spiral turbulence is of great interest, mainly because studies of fibrillation in cardiac tissue show a close relationship between the disease and the onset of spiral turbulence [2,5,9–11]. From an experimental point of view, the Belousov-Zhabotinsky (BZ) reaction-diffusion system is one of the most convenient model systems to experimentally study the mechanism of this phenomenon, for this much simpler system supports spiral waves and can be studied systematically. It may reveal certain universal critical behaviors that are shared with the cardiac tissue and other nonlinear systems that can be considered as reaction-diffusion systems.

In the recent decade, studies of the transitions to spiral turbulence have witnessed significant progress. Spiral instabilities in quasi-two-dimensional (quasi-2D) systems, such as the Eckhaus instability, Doppler instability, and line defect development, have been identified [12–14]; different control strategies have been discussed in theory [6,7,16,17]. In the 3D regime, scroll-wave (SW) instabilities have been the subject of many simulation studies [3,5,8,15,18–21], but few experiments [8,15] have been carried out in open systems to investigate its asymptotical behavior and to verify the numerical results. In the field of controlling spiral turbulence, despite some attempts [16], so far no successful control has been reported in experiments.

Recently, a mechanism of SW instability and its control was proposed in a theoretical study [5,18,19]. The process is much like Winfree turbulence that is caused by negative-tension instability (NTI) [2,5]. In a numerical study and theoretical analysis, Alonso *et al.* [5,18,19] found that introducing a global periodic forcing to a reaction-diffusion system can suppress the Winfree turbulence.

In this paper, we report an experimental result on successfully controlling a SW collapse in a 3D BZ system with gradients. Here, we try to stabilize the SW observed earlier [8] using the control strategy of a periodic forcing. The control is effective, but deviates from a previous theoretical prediction. This forced us to seek a different theoretical explanation. With the help of numerical simulations and theoretical analysis, we found that the mechanism of control can be well understood by modulating the phase twist of the SW.

II. EXPERIMENT

The experiments were carried out in a spatial open reactor similar to that used in previous studies [15]. The reaction medium is a 0.4-mm-thick porous glass (22 mm in diameter, made of Vycor glass 7390, Corning), sandwiched between two continuously fed stirred tank reactors (CSTRs) (I) and (II), so that its boundary conditions can be fixed. Ferroin-catalyzed BZ reaction with a small quantity of $Ru(bpy)_3^{2+}$ [tris(2,2′-bipyridyl)dichlororuthenium(II) hexahydrate] was chosen. The $Ru(bpy)_3^{2+}$ makes the system light sensitive, so that an external forcing can be applied. A light projector (Sony, VPL-PX11), whose illumination intensity is controlled by a computer and measured by a luminometer (Handy, ST-85), was used as the source of external forcing. Two-dimensional projections of the patterns were registered by a charged-coupled-device (CCD) camera. The data were recorded in another computer via a frame grabber.

Different chemical reactants were fed into CSTRs (I) and (II) so that there existed concentration gradients across the reaction medium. A patterned layer that supports spiral waves formed inside the medium. According to previous studies [15,21], the increase of the concentration of sulfuric acid in reservoir(I) ($[H_2SO_4]^I$) in a chosen regime will thicken the patterned layer, turning a quasi-2D system to an actually 3D one. Therefore the observed spiral pattern has a 3D feature and the spiral center is a filament. According to our previous study, SWs can be spontaneously created in this gradient system; they eventually collapse when the chemical gradients reach a critical value [8]. In the experiments, we intentionally set the experimental condition in this regime, so that both filament and scroll ring were observed, and similar

*These authors contributed equally to this work.
†Corresponding author. qi@pku.edu.cn

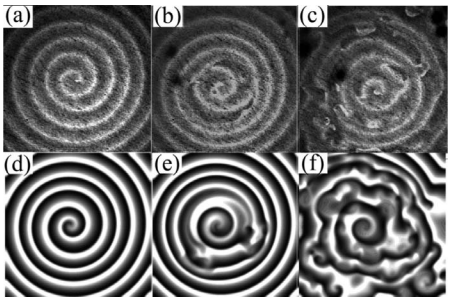

FIG. 1. Snapshots illustrating the transition from a stable SW to the onset of its collapse and to the turbulent state: (a)–(c) experiment. $[H_2SO_4]^I$: (a) 0.495 M, the stable SW; (b) 0.505 M, the onset of SW collapse; (c) 0.510 M, the turbulent state. ω_e=0.36 rad s^{-1} and I_f=2800*l*x. (d)–(f) Simulation corresponding to (a)–(c), respectively. a_{20}: (d) −0.135, (e) −0.134, and (f) −0.131. ω_s =0.28 rad t.u.$^{-1}$ and a_f=0.006. Other parameters as described in text. The region shown in (a)–(c) is 11.5×11.5 mm^2; the area of (d)–(f) has a size of 512×512 grids.

3D characters were confirmed in both experiments and simulations, which will be shown below. In the study, $[H_2SO_4]^I$ was chosen as one of the control parameters. Other parameters were kept fixed: $[NaBrO_3]^{I,II}$=0.2 M, $[CH_2(COOH)_2]^I$=0.6 M, $[KBr]^I$=60 mM, $[H_2SO_4]^{II}$ =0.2 M, $[Ferroin]^{II}$=0.917 mM, and $[Ru(bpy)_3^{2+}]^{II}$ =0.083 mM. The reaction temperature was 24±0.5 °C.

In the experiments, the forcing was spatially uniform, but temporally periodic: $I_t=I_0+I_f\cos(\omega_e t)$, where I_0 was fixed at 4200 lx, and I_f was set at 2800 lx for "strong forcing" and 800 lx for "weak forcing." The frequency of periodic forcing (ω_e) was the other control parameter besides $[H_2SO_4]^I$. $[H_2SO_4]^I$, which determines the gradient of $[H_2SO_4]$, could be changed from 0.48 M to 0.54 M with a precision of 0.005 M; ω_e varied from 0.157 rad s^{-1} to 0.393 rad s^{-1} with an interval of 0.0075 rad s^{-1}. The rotating frequency ω_0 of SWs was measured as about 0.206±0.003 rad s^{-1} just before the onset of its collapse. We should point out that in general the external periodic forcing will cause the spiral tip or filament meandering. However, because the external forcing that we use was weak, we found that this complex filament motions could safely ignored.

Figures 1(a)–1(c) show, respectively, a snapshot of a stable SW, the onset of its collapse, and the turbulent state. When $[H_2SO_4]^I$ is set at low values (0.48 M), the initial SW is stable [Fig. 1(a)]. The structure of SW is hardly recognizable in the image of projection, but a previous study confirmed its existence [8]. To get each critical value of $[H_2SO_4]_c^I$ for the onset of SW collapse, we fix the value of ω_e and increase 0.005 M in stepwise on $[H_2SO_4]^I$, until the SW collapses [Fig. 1(b)] and the turbulence dominates the whole system [Fig. 1(c)]. In each step we let the SW relax for around 1*h* to make sure the chemical waves attain their asymptotic state. Repeating this process for other values of ω_e, we obtained every $[H_2SO_4]_c^I$ for different ω_e.

Figure 2(a) provides a phase diagram of the SW-turbulence transition. One observes that $[H_2SO_4]_c^I$ undulates between 0.49 M and 0.52 M when SWs are under the strong forcing, while $[H_2SO_4]_c^I$ is fixed at 0.50 M when SWs are

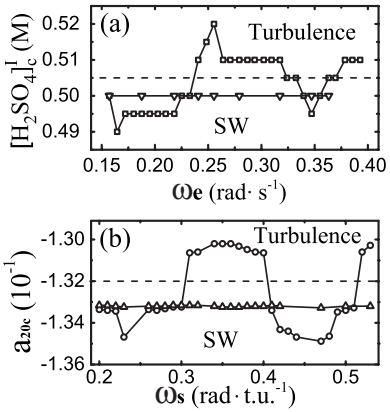

FIG. 2. Plots indicate the onset of SW collapse in the control parameter plane. (a) Experiments. I_f: □, 2800 lx; ▽, 800 lx; dashed line, 0. (b) Simulations. a_f: ◯, 0.006; △, 0.003; dashed line, 0. Other parameters are the same as Fig. 1.

under the weak forcing. In comparison, without forcing $[H_2SO_4]_c^I$ is 0.505 M. This indicates that weak forcing does not help to enhance SW, while strong forcing has a stability effect on SWs only in certain frequency regions. Another observation is that the phenomena of the SW collapse in nonenhancing cases are completely different from those in enhancing cases (in Fig. 2, enhancing cases are above the dashed lines, and nonenhancing are below those; see movies in supplementary material [22]). In the former cases the SW collapse always comes after the appearance and the breakup of scroll rings [8] (we call them the first collapse). In the latter cases, the collapses, which are similar with the turbulence observed in Refs. [7,12], are more likely due to the convective instability and have no relationship with the gradient effect. We confirmed them by our 2D simulations (we call them the second collapse). This indicates that a suitable periodic forcing can eliminate the first collapse and keep a SW stable until the onset of convective instability. In the theoretical part of the paper, our analysis will focus on the first collapse.

According to Ref. [5], the forcing frequency can be separated by the rotating frequency ω_0 of SWs, below or above which the forcing will weaken or enhance the stability of SWs. In contrast, our experiments indicate that the enhancing and weakening effects appear alternately as ω_e consecutively increases and ω_0 is not a dividing value. Furthermore, the stability enhancement only appears in the strong forcing case; the weak forcing influences the stability of SWs just a little. These results force us to seek a new explanation. In the following we present the results of our model simulations, together with a theory to explain the observed phenomena.

III. SIMULATION

Our simulations were conducted using the FitzHugh-Nagumo model, which is similar to that in Ref. [8]:

$$\frac{\partial u}{\partial t} = u(1-u)[u-a(z,t)] - v + \nabla^2 u, \qquad (1)$$

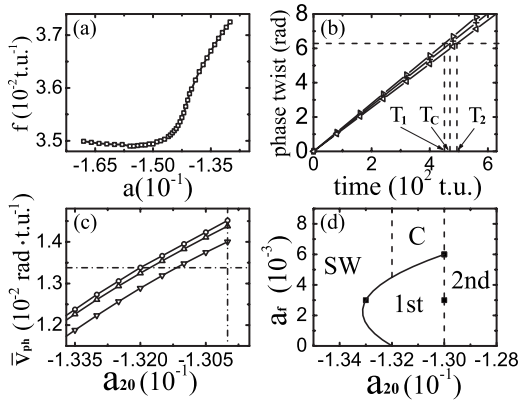

FIG. 3. (a) The rotation frequency f of a 2D spiral-wave system as a function of the parameter a. (b) Plots of the phase twist vs time in unforced systems. v_{ph}: △, 0.013 95; +, 0.013 38; ▽, 0.01273. (c) The average rate of the phase twist $\bar{v}_{ph}$ vs a_{20}. a_f: ◯, 0; △, 0.003; and ▽, 0.006; the dashed line illustrates the value of v_{phc}. (d) A plane of phase diagram. C means controllable.

$$\frac{\partial v}{\partial t} = \varepsilon(u - v), \tag{2}$$

where u and v are the diffusible activator and in-diffusible inhibitor, respectively, and $\nabla^2 = \partial^2/\partial x^2 + \partial^2/\partial y^2 + h\partial^2/\partial z^2$. To mimic the reaction medium in the experiment, the z direction of the Cartesian coordinates system is represented by the coupling of 20 layers of the 2D system (grid size 512×512) together and h decides the coupling strength in this dimension. We applied a simple Euler method and non-flux-boundary condition in the simulations, with a time step of $dt=0.03$ (time unit) and a space step of 1 (space unit). We fixed $\varepsilon=0.08$ and $h=0.32$. The initial state was a single SW as in the experiment.

The values of a in the model were assigned as $a(z,t) = a_i + a_f \sin(\omega_s t)$ $(i=1,2,\ldots,20)$, in which $a_i = a_{i-1} + 1.053 \times 10^{-3}$, describing the gradient character of the system; a_f and ω_s represent, respectively, the amplitude and frequency of homogenous periodic forcing. The whole system can be determined by a_f, a_{20} and ω_s. To compare with the experiment a_f was set at 0.006 for strong forcing and 0.003 for weak forcing. a_{20} increased gradually from −0.138. As stated below in the text corresponding to Fig. 3(a), this simulates the increase of the gradient effect, which influences the stability of SWs [8]. Also, we will see later that the key factor of our system is the gradient effect. Therefore, to explain our results by using the FitzHugh-Nagumo model with a similar gradient is warranted. The range of ω_s was from 0.20 rad t.u.$^{-1}$ to 0.52 rad t.u.$^{-1}$ (t.u. means time unit of our simulation). The rotating frequency ω_0' of SWs under this condition was measured as about $0.23 \cdot$t.u.$^{-1}$ just before onset of its collapse. As in the experiments, we carefully checked the influence of the external forcing on the spiral tip or filament motion. We found that the filaments' complex motion, such as meandering led by the periodic forcing, was small and could be neglected.

Figures 1(d)–1(f) show three typical patterns corresponding to Figs. 1(a)–1(c). As observed in the experiments, the increase of the gradient effect (a_{20}) triggers the SW-turbulence transition. The SW is stable when a_{20} is small enough [$a_{20}=-0.137$, Fig. 1(d)]. When a_{20} is slowly increased to reach a critical value, the SW begins to collapse [$a_{20}=-0.132$, Fig. 1(e)]. The turbulent state will eventually dominate the whole system [$a_{20}=-0.131$, Fig. 1(f)]. We repeated this process with different forcing amplitude and frequency to get critical values of $a_{20c}(a_f, \omega_s)$. The resulting phase diagram is presented in Fig. 2(b). The simulation results qualitatively agree with the experiments: the onset of the transition does not qualitatively change in the weak forcing ($a_f=0.003$) case, where the turbulence takes place via the first-type collapse of the SW; with a large forcing amplitude ($a_f=0.006$), the enhancing and weakening effects on the stability of SW appear alternately as ω_s consecutively varies and SW collapse changes to the second type in enhancing cases.

IV. THEORETICAL ANALYSIS

As proved in Ref. [8], the first type collapse is due to the different rotation frequencies of 2D spirals in different layers of the gradient system, which cause a phase twist. The twist can be measured by the phase difference between the top and bottom layers. Figure 3(a) shows the frequency (f) of the spiral versus control parameter a in the 2D system without forcing. Because of the nonlinear relationship between the frequency of the 2D spiral and the control parameter a, in the corresponding 3D gradient system, the gradient in the control parameter a can be translated into a frequency gradient. When we increase a_{20} in our simulations, the frequency gradient increases. According to this, we see that when a_{20} in 3D systems is approaching the turning point (around −0.145), the difference in frequencies between the top and bottom layers is becoming larger. When the twist accumulates to reach 2π, the coupling effect removes a twist by shifting a wavelength (called a phase shift). The shifting frequency F has a linear relation with $f(a_{20}) - f(a_1)$, as shown in the Fig. 6(b) of Ref. [8]. According to these, the rate of twist (v_{ph}) can be defined as $v_{ph}(a_{20}) = 2\pi F = 2\pi\alpha[f(a_{20}) - f(a_1)] + \beta$, while $\alpha \approx 1$ and β is a constant determined by the system. The corresponding twisting time T when phase twist accumulates from 0 to 2π is $2\pi/v_{ph}$. In our analysis, we assume that there exists a critical T_c, such that if $T < T_c$, the system cannot renew in time so that first collapse happens. This applies to the unforced and forced systems. Figure 3(b) gives three cases of phase twist accumulations in the unforced systems: $T=T_c$, the critical case; $T_1 > T_c$, where SW collapses; and $T_2 < T_c$, where SW remains stable. When the critical value of a_{20c} (=−0.132) is identified in Fig. 2(b), one can obtain v_{phc} (=0.013 36) from Fig. 3(c) (explained in the next paragraph) and then obtain T_c using $T_c = 2\pi/v_{phc}$.

When the periodic forcing on $a(z,t)$ is added, v_{ph} also depends on t, such that it oscillates between $v_{ph}(a_{20} - a_f)$ and $v_{ph}(a_{20} + a_f)$. We define $\bar{v}_{ph}$ as the average value of v_{ph} in a period, which is a function of a_{20} and a_f. Figure 3(c) shows the calculation result of $\bar{v}_{ph}$ for different value of a_f, obtained from data of Fig. 3(a) with $\alpha=1$ and $\beta=0$. The values of α and β are inessential in our explanation. In weak forcing cases ($a_f=0.003$), the value of $\bar{v}_{ph}$ is similar to that without

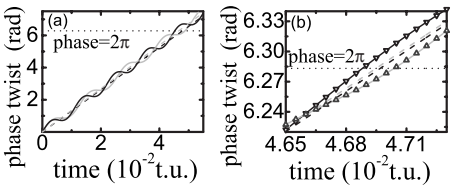

FIG. 4. Phase accumulation of the phase twist as a function of time. (a) Schematic plot and (b) actual calculation. The gray dashed line corresponds to the critical case of nonforcing; the black dashed line is calculated from the average rate of the twist $\bar{v}_{ph}$; the black curve [with $\triangledown$ in (b)] corresponds to the case of $T<T_c$; the gray curve [with $\triangle$ in (b)] corresponds to the case of $T>T_c$.

forcing. As a_{20} grows, $T<T_c$ eventually happens and the SW collapses. In fact, the lowest T is determined by $v_{ph}(a_{20}+a_f)$ rather than $\bar{v}_{ph}$; this explains that the weak forcing weakens instead of enhances the SW, as observed in both the experiments and simulations.

As the amplitude of period forcing increases, the value of $\bar{v}_{ph}$ becomes lower due to nonlinear responses of the system to the external forcing [see Fig. 3(b)]. This effect helps to stabilize the SW. However, when its value is close to v_{phc}, the accumulating time T of the phase twist is strongly influenced by its oscillatory nature. Figures 4(a) and 4(b) present, respectively, a schematic and the actual calculation result of the phase twist curve versus time in the system with strong forcing. The latter is acquired by numerical integral of v_{ph} on t. One observes that the curve is not a straight line, but oscillates up and down around the line whose slope is $\bar{v}_{ph}$. In this situation, the twisting time T is determined not only by the $\bar{v}_{ph}$, but also by the phase of the oscillation when the twist reaches 2π. As shown in Fig. 4, with a right frequency of external forcing, the intersection is at the right side of the average straight line [gray curve in Fig. 4(a) and $\triangle$ in Fig. 4(b)]. In this case $T>2\pi/\bar{v}_{ph}$ and it is possible for the system to remain $T>T_c$ even when $\bar{v}_{ph}$ is a little larger than v_{phc}. On the other hand, a wrong frequency of external forcing will make the intersection at the left side, so that $T<T_c$ and SWs collapse [black curve in Fig. 4(a) and $\triangledown$ in Fig. 4(b)]. These explain the undulating nature of the turbulence onset in Fig. 2. Here we assume that the initial phases of curves are the same (e.g., $\text{phase}_0=0$ in Fig. 4); this is justified because a phase shift periodically happens in stable SWs and there exists a phase locking between external forcing the response of the system. Figure 3(d) provides a plane of the phase diagram of the system. The controllable region is on the upper middle part of the diagram. Based on this analytical picture, we predict that when $\bar{v}_{ph}$ is near v_{phc}, an abrupt change of the phase of the periodic forcing can alter the stability of the SW. This prediction has been confirmed in our simulation.

V. CONCLUSION

In conclusion, we report an experimental realization of controlling spiral turbulence. The experimental results are in good agreement with our theoretical analysis. Our results show an effective way to control one type of spiral turbulence in a 3D reaction-diffusion system with gradient. The theoretical analysis not only explains the observed phenomena, but also points out a control mechanism that is different from the strategy discussion in Refs. [5,18,19]. All these provide a possible way to suppress first type SW destabilization. Together with a strategy to suppress convective instability of spiral waves [7], we believe the spiral turbulence in this system can be avoided.

ACKNOWLEDGMENTS

This work is partially supported by the NSF of China and MOST of China. Y.W. thanks the National Foundation for Fostering Talents of Basic Science (Grant No. J0630311) and Peking University (President Grant) for support.

[1] Q. Ouyang and H. L. Swinney, Chaos **1**, 411 (1991).
[2] A. T. Winfree, Science **266**, 1003 (1994).
[3] S. Mironov, M. Vinson, S. Mulvey, and J. Pertsov, J. Chem. Phys. **100**, 1975 (1996).
[4] M. Kim *et al.*, Science **292**, 1357 (2001).
[5] S. Alonso, F. Sagués, and A. S. Mikhailov, Science **299**, 1722 (2003).
[6] X. N. Wang, Y. Lu, M. X. Jiang, and Q. Ouyang, Phys. Rev. E **69**, 056223 (2004).
[7] M. X. Jiang, X. N. Wang, Q. Ouyang, and H. Zhang, Phys. Rev. E **69**, 056202 (2004).
[8] C. Wang, S. Wang, C. X. Zhang, and Q. Ouyang, Phys. Rev. E **72**, 066207 (2005).
[9] R. A. Gray *et al.*, Science **270**, 1222 (1995).
[10] F. Fenton and A. Karma, Chaos **8**, 20 (1998).
[11] A. V. Panfilov, Chaos **8**, 57 (1998).
[12] L. Q. Zhou and Q. Ouyang, Phys. Rev. Lett. **85**, 1650 (2000).
[13] Q. Ouyang, H. L. Swinney, and G. Li, Phys. Rev. Lett. **84**, 1047 (2000).
[14] J. S. Park and K. J. Lee, Phys. Rev. Lett. **83**, 5393 (1999).
[15] C. X. Zhang, H. M. Liao, and Q. Ouyang, J. Phys. Chem. B **110**, 7508 (2006).
[16] H. M. Liao, L. Q. Zhou, C. X. Zhang, and Q. Ouyang, J. Phys. Chem. B **108**, 10192 (2004).
[17] H. Zhang, J. X. Chen, Y. Q. Li, and J. R. Xu, J. Chem. Phys. **125**, 204503 (2006).
[18] S. Alonso, F. Sagués, and A. S. Mikhailov, J. Phys. Chem. A **110**, 12063 (2006).
[19] S. Alonso, F. Sagués, and A. S. Mikhailov, Chaos **16**, 023124 (2006).
[20] U. Storb, C. R. Neto, M. Bär, and S. C. Müller, Phys. Chem. Chem. Phys. **5**, 2344 (2003).
[21] C. Zhang, H. Zhang, Q. Ouyang, B. Hu, and G. H. Gunaratne, Phys. Rev. E **68**, 036202 (2003).
[22] See EPAPS document No. E-PLEEE8-77-013804 for movies of various phenomena in experiment and simulation. For more information on EPAPS, see http://www.aip.org/pubservs/epaps.html.